ORIGINAL ARTICLE

JBMR

Wdr5 Is Required for Chick Skeletal Development

Shimei Zhu,[1*] Eric D Zhu,[1*] Sylvain Provot,[2] and Francesca Gori[1]

[1]Endocrine Unit, Massachusetts General Hospital, Harvard Medical School, Boston, MA USA
[2]Department of Anatomy, University of California San Francisco, San Francisco, CA USA

ABSTRACT

Wdr5, a bone morphogenetic protein 2 (BMP-2)–induced protein belonging to the family of the WD repeat proteins, is expressed in proliferating and hypertrophic chondrocytes of the growth plate and in osteoblasts. Although previous studies have provided insight into the mechanisms by which Wdr5 affects chondrocyte and osteoblast differentiation, whether Wdr5 is required in vivo for endochondral bone development has not been addressed. In this study, using an avian replication competent retrovirus (RCAS) system delivering Wdr5 short hairpin (sh) RNA to silence Wdr5 in the developing limb, we report that reduction of Wdr5 levels delays endochondral bone development and consequently results in shortening of the skeletal elements. Shortening of the skeletal elements was due to impaired chondrocyte maturation, evidenced by a significant reduction of Runx2, type X collagen, and osteopontin expression. A decrease in Runx2, type collagen I, and ostepontin expression in osteoblasts and a subsequent defect in mineralized bone was observed as well when Wdr5 levels were reduced. Most important, retroviral misexpression of Runx2 rescued the phenotype induced by Wdr5 shRNA. These findings suggest that during limb development, Wdr5 is required for endochondral bone formation and that Wdr5 influences this process, at least in part, by regulating Runx2 expression. © 2010 American Society for Bone and Mineral Research.

KEY WORDS: WDR5; RCAS; shRNA; ENDOCHONDRAL BONE FORMATION; CHICKEN LIMB

Introduction

Long bones of the appendicular skeleton are formed by a process known as endochondral bone ossification, in which mesenchymal cells differentiate into chondrocytes and then undergo a series of changes that include proliferation, differentiation into hypertrophic chondrocytes, mineralization of the cartilage matrix, apoptosis of the hypertrophic chondrocytes, vascular invasion, and formation of an ossification center containing type I collagen–expressing osteoblasts.[1–5] This complex process is regulated by crosstalk among several transcription factors and signaling molecules expressed in and secreted by developing chondrocytes and osteoblasts.[4–11]

The chicken limb bud is a classic model for studying the mechanisms that regulate skeletal development.[11–14] The limb buds become visible around Hamilton and Hamburger (HH) stages 18 to 20 (E3–3.5), and limb patterning takes place in the following 2 days. At this early stage, the limb bud consists of mesenchymal condensations surrounded by ectodermal cells. Cells within the condensations begin to differentiate into cartilage, and in the following 3.5 days, endochondral ossification occurs, leading to the formation of bone tissue within the cartilage template. By E10, chondrocytes in the growth plate and osteoblasts become evident.

Investigations using the chick embryos and the Rous sarcoma virus (RSV)–derived replication-competent avian retroviral (RCAS) vectors[15] have had a crucial impact on elucidating the mechanisms regulating the cellular and molecular bases of skeletal development, such as patterning and outgrowth of the limb, developmental regulation of endochondral bones, and cranial skeletal development.[11,16–27] One of the major strengths of the avian RCAS approach is the ability to misexpress a gene in vivo in a sustained fashion, followed by analyses of the biologic consequences of this misexpression on skeletal development.

Wdr5 is a member of a family of structurally conserved proteins, the WD repeat proteins.[28–31] The common function of these proteins is to form a scaffold for protein-protein interaction and to coordinate numerous cellular functions, such as signal transduction, cell cycle, apoptosis, and transcription regulation.[29,31] In mice, Wdr5 is expressed developmentally in chondrocytes and osteoblasts, and stable expression of Wdr5 in these cells accelerates the program of chondrocyte and osteoblast differentiation.[32,33] Targeted expression of Wdr5 to mature osteoblasts accelerates osteoblast differentiation at least in part by enhancing the canonical Wnt signaling pathway[34] and promotes chondrocyte differentiation by modulating the expression of Twist-1.[35] Consistent with these findings, when Wdr5 protein is reduced using siRNA technology in MC3T3E-1

Received in original form December 7, 2009; revised form April 8, 2010; accepted May 21, 2010. Published online June 7, 2010.
Address correspondence to: Francesca Gori, PhD, 50 Blossom Street, Boston, MA 02114, USA. E-mail: gori@helix.mgh.harvard.edu
*The first two authors contributed equally to this work.

Journal of Bone and Mineral Research, Vol. 25, No. 11, November 2010, pp 2504–2514
DOI: 10.1002/jbmr.144

cells, which derived from calvarial osteoblasts, these cells fail to differentiate into mature osteoblasts expressing osteocalcin and depositing mineralized matrix,[36] demonstrating that, at least in vitro, Wdr5 is needed for the differentiation of osteoblasts into mature osteoblasts.

Although our previous studies have shown that Wdr5 induces chondrocyte and osteoblast differentiation in vitro and in vivo, whether Wdr5 is required for endochondral ossification in vivo has not been addressed. Because the molecular mechanism underlying skeletal development in chickens is applicable to other vertebrates and all genes found to regulate skeletal development in chicks have been described to play the same function in mice,[16,37–40] investigations using the avian system will be informative to further explore the role of Wdr5 in skeletal development in mammals. Here, to investigate the functional role of Wdr5 during endochondral bone formation, loss-of-function studies using RCAS-mediated delivery of shRNA targeting Wdr5 were performed to silence Wdr5 during chicken limb development.

Material and Methods

siRNA design and construction of retroviral constructs

Three different shRNAs (1 to 3) targeting the chicken Wdr5 cDNA sequence and one scrambled shRNA control were designed. These shRNAs were subcloned into the pSilencer 2.0-U6 siRNA expression vector (Ambion, Austin, TX, USA) downstream from the U6 RNA polymerase III (U6 Pol III) promoter. PCR analysis was performed to generate Cla I sites 5′ and 3′ to the cassette containing the U6 Pol III shRNA for cloning into the pGEM shuttle vector (Promega, Madison, WI, USA). ClaI digestion of the pGEM shuttle vectors followed by ligation of the four cassettes containing the U6 Pol III shRNAs and RCAN vector of subgroup B [RCAN(B); kindly provided by Dr Tabin, Harvard Medical School, Boston, MA, USA] were performed to generate three RCAN(B) vectors containing the selected Wdr5 shRNA sequences [RCAN(B)-1, -2, and -3] and one RCAN(B) vector containing a scrambled shRNA [RCAN(B)-S].

Propagation, titration and injection of RCAN(B) virus

High-titer (>1 to 5×10^8 IU/mL) RCAN(B)-1, -2, -3, and -S, as well as RCAS(A)-GFP (provided by Dr Tabin, Harvard Medical School) and RCAS(A)-chRunx2 viruses (provided by Dr Mundlos, Max Plank Institute for Molecular Genetics, Berlin, Germany) were generated by standard procedures.[41,42] Viral infection was assessed using the 3C2 monoclonal antibody (Developmental Studies Hybridoma Bank of the University of Iowa, Iowa City, IA, USA). High-titer viruses were injected into the right wings of HH stage 18 to 21 (E3.0–3.5) chick embryos. Uninfected left wings were used as controls. To ensure viral infection throughout the cartilage elements, limb buds were injected in the anteroposterior regions of the distal margin. To assess the effects of Wdr5 downregulation, chick embryos were harvested at multiple developmental stages [between HH stages 35 (E8.5) and 38 (E12)], and proximal and distal skeletal elements of the wings were analyzed. For coexpression experiments, high-titer RCAN(B) viruses expressing shWdr5 and high-titer RCAS(A) viruses expressing Runx-2 or GFP were used. RCAS viruses belonging the subgroup A were used in coinjection experiments to avoid viral interference, a mechanism by which a subgroup of viruses can block other members of the same subgroup from superinfecting the same host cell.[26,42] For these experiments, RCAN(B)-1, -2, -3, and -S and RCAS(A)-GFP of RCAS(A)-chRunx-2 viruses were used in 1:1 ratio mix.

Alcian blue and alizarin red staining

HH stage 36 (E10) and stage 38 (E12) embryos were incubated in a solution of 80% ethanol and 20% acetic acid containing 0.015% alcian blue 8GX (Sigma, St Louis, MO, USA). Embryos were dehydrated in 100% ethanol and then incubated in 0.5% KOH containing 0.01% alizarin red (Sigma). After 24 hours, embryos were cleared in 1% KOH containing 20% glycerol and then sequentially incubated in 0.5% KOH containing increasing concentrations of glycerol (20%, 40%, and 80%).

Histologic evaluation

Infected right wings and uninfected left wings were fixed in 4% paraformaldehyde (PFA). After 24 hours, specimens were transferred to a 5% sucrose solution, followed by incubation in 30% sucrose. Specimens then were embedded for frozen sections. Tissue blocks were cut into 5-μm sections and stained with hematoxylin or toluidine blue to permit phenotypic analyses.

BrdU incorporation

Then 400 mL of 1 mM BrdU was added by opening a window in the eggshell of the embryos at stage HH 36 (E10). After 3 hours, the embryos were harvested, and infected right wings and uninfected left wings were isolated and processed for frozen sections. BrdU-positive nuclei were detected using a Zymed Immunostaining Kit (Zymed, San Francisco, CA, USA) according to the manufacturer's instructions. BrdU-positive and BrdU-negative nuclei were counted in nine similarly sized regions of each of the round and columnar proliferating regions of uninfected left wings and infected right wings. Data were expressed as percent positive nuclei in the selected areas.

Whole-mount immunohistochemistry analyses

Embryos were harvested at HH stage 25 (E5) and incubated in 4% PFA overnight. Immunostaining for RCAN vector was performed using the 3C2 monoclonal antibody (Developmental Studies Hybridoma Bank of the University of Iowa). Immunoreactive proteins were visualized using 0.5 mg/mL of 3-3′-diaminobenzidine (DAB; Sigma) and 0.03% H_2O_2.

Immunohistochemistry analyses

Immunohistochemistry analyses were performed using α-Wdr5,[32] anti-CD31 (BD Biosciences, Franklin Lakes, NJ, USA), or a nonspecific rabbit and mouse IgG (Sigma). Immunoreactive proteins were visualized using the TSA Biotin System Kit (PerkinElmer, Boston, MA, USA) or the EnVison G/2 System/AP Rabbit/Mouse (Permanent Red, DakoCytomation, Carpinteria, CA, USA) according to the manufacturer's instructions.

Immunoreactive proteins were visualized using Streptavidin HRP & Streptavidin Texas Red (PerkinElmer).

Western blot analyses

To evaluate Wdr5 silencing, infected right wings and uninfected left wings were isolated at HH stages 35 (E8.5), 36 (E10), and 38 (E12) and dissected free of adjacent tissue under a dissecting microscope. The distal and proximal skeletal elements of the wings then were homogenized, and 2 μg of total protein was subjected to SDS-PAGE under reducing conditions. Membranes were incubated with α-Wdr5 and α-actin (Santa Cruz Biotechnology, Inc., Santa Cruz, CA, USA). Immunoreactive proteins were visualized using a chemiluminescence detection kit (NEN, Boston, MA, USA) according to the manufacturer's instructions.

Histomorphometry

Histomorphometric analyses on ulnas isolated from HH stage 38 (E12) embryos infected with RCAN(B)-1 plus RCAS(A)-chRunx2 or RCAN(B)-1 plus RCAS(A)-GFP were performed with the Osteomeasure System (Osteometrics, Inc., Atlanta, GA, USA) using standard procedures. Cortical bone was measured in uninfected left and infected right ulnas. Data were expressed as percent of cortical bone per total area of the ulna in the same sample.

In situ hybridization analyses

Digoxigenin (DIG)– or ^{35}S-UTP-labeled probes specific for the chicken Sox9, type X collagen, type II collagen, type I collagen, Runx-2, and osteopontin mRNAs were used for in situ hybridization, as described previously.[34,35]

Quantitative real-time PCR

Total RNA was prepared from HH stage 36 (E10) and stage 38 (E12) skeletal elements isolated from infected right and uninfected left wings that had been dissected free of adjacent tissue under a dissecting microscope using the RNeasy Plus Mini Kit (Qiagen, Valencia, CA, USA). cDNA was synthesized using Superscript II reverse transcriptase (Invitrogen). Quantitative real-time PCR was performed using the Opticon DNA Engine System (MJ Research, Waltham, MA, USA). mRNA levels encoding each gene of interest were normalized for GAPDH mRNA in the same sample using the formula of Livak and Schmittgen.[43]

Von Kossa staining

Sections of infected right wings and uninfected left wings were incubated in 5% silver nitrate solution and exposed to a 60-W electric light bulb for 5 to 15 minutes. Slides then were washed several times in distilled water, followed by incubation in 2.5% sodium thiosulfate for 30 seconds.

Statistical analyses

All values are expressed as mean ± SEM, and a Student's paired t test was used to compare differences between the infected right wings and uninfected control wings. For quantitative real-time PCR, the expression of selected genes was normalized to that of GAPDH in the same sample. Values were expressed as the relative expression of the normalized mRNAs levels of the infected right wings versus that of uninfected left wings at each time point. A p value of less than .05 was considered statistically significant. All experiments were performed using at least four chicken embryos.

Results

Wdr5 is expressed in proliferating and hypertrophic chondrocytes and in osteoblasts during endochondral ossifications

The expression of Wdr5 in the developing cartilage elements was assessed on sections of wings isolated from HH stage 36 (E10) and stage 38 (E12) embryos. These time points were chosen because the proliferative prehypertrophic and hypertrophic chondrocytes as well as osteoblasts can be well evaluated. Consistent with the expression pattern of Wdr5 during mouse endochondral bone development,[33,34] in chicken limbs, Wdr5 is expressed in proliferating and hypertrophic chondrocytes as well as in the perichondrium and the periosteum (Fig. 1). Wdr5 expression in these cell types was confirmed by in situ analyses for type I collagen (ColII), type I collagen X (ColX), and osteopontin (OP) (Fig. 1). No signal was detected when nonspecific rabbit IgG was used, confirming specificity of the signal (Fig. 1). As shown in Fig. 1, Wdr5 expression is not restricted to chondrocytes and osteoblasts, but Wdr5 is also expressed in muscles and skin, confirming previous findings demonstrating that ubiquitous expression of Wdr5.[32] The findings that the expression pattern of Wdr5 in chicken limb mirrors that in mice indicate that studies in the chicken system will be informative to address whether Wdr5 is required for endochondral ossification in mammals.

Retroviral expression of Wdr5 shRNAs reduces endogenous Wdr5 levels in chondrocytes and osteoblasts

The expression of Wdr5 in chondrocytes and osteoblasts is consistent with a role for Wdr5 in influencing endochondral bone formation. To address whether Wdr5 is required for endochondral ossification, loss-of-function studies were performed. To this purpose, an avian replication-competent ASLV LTR, (RCAS) system delivering a Wdr5 short hairpin RNA (shRNA) sequence was used to silence Wdr5 levels in the developing chicken limb.

Three RCAN(B) viruses expressing three selected Wdr5 shRNA sequences [RCAN(B)-1, RCAN(B)-2, and RCAN(B)-3 and one RCAN(B) vector containing a control scrambled shRNA (RCAN(B)-S] were used. To visualize the location and extent of viral infection, HH stage 18 to 20 (E3–3.5) right limb buds were infected with RCAN(B)-shWdr5 viruses [RCAN(B)-1, -2, and -3]. Embryos then were harvested at HH stage 25 (E5), and sections of infected and uninfected wings were subjected to whole-mount immunohistochemistry analyses for the RCAN protein. As shown in Fig. 2A, extensive viral infection was obtained in the injected wings.

To quantify the silencing efficiency of the shRNAs, HH stage 18 to 20 (E3–3.5) right limb buds were infected with high titers of either the RCAN(B)-shWdr5 viruses [RCAN(B)-1, -2 and -3] or the

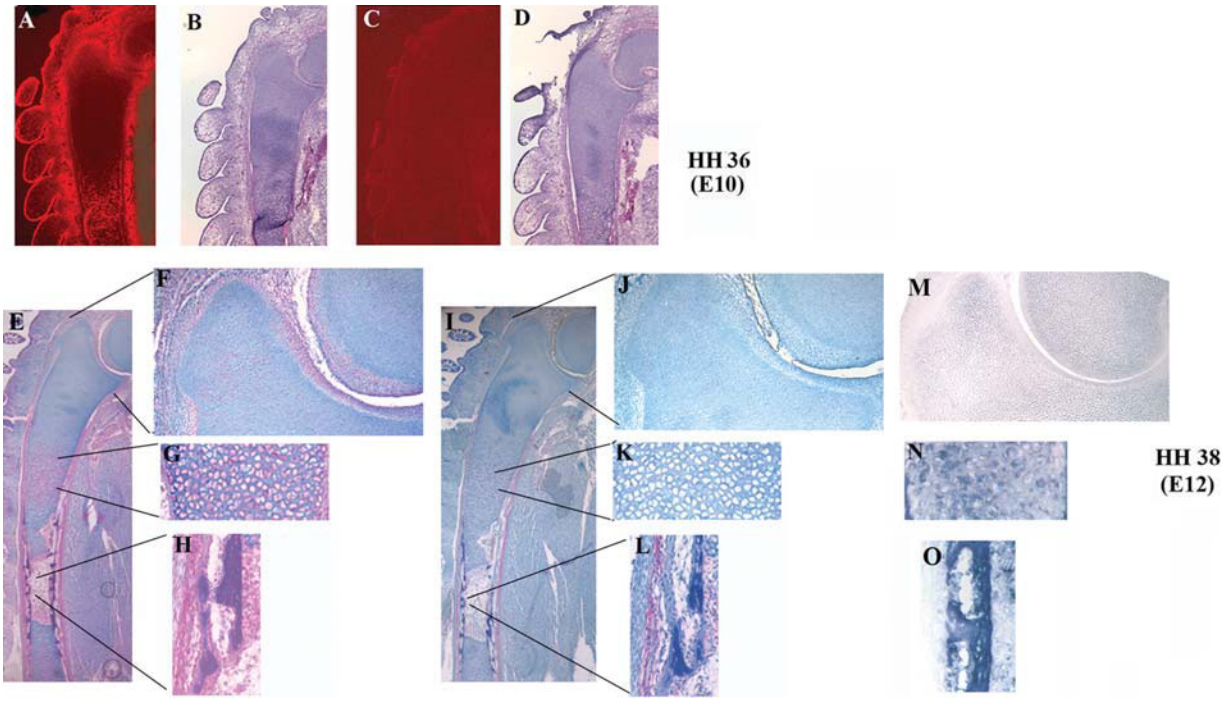

Fig. 1. Expression of Wdr5 during chick endochondral ossification. Immunohistochemical analyses were performed using an α-Wdr5 (*A, E*) or a nonspecific IgG (*C, I*). (*A–D*) HH stage 36 (E10) wings. Immunoreactive proteins were visualized using streptavidin Texas red. (*B, D*) Sections were counterstained with hematoxylin and eosine (*H&E*). (*E –L*) HH stage 38 (E12). Inserts indicate the expression of Wdr5 (in red) in the proliferating (*F*) and hypertrophic chondrocytes (*G*) and in the periosteum (*H*). Sections were counterstained with hematoxyline. (*M–O*) In situ hybridization analyses for ColII (*M*), ColX (*N*), and OP (*O*). Representative ulnas are shown; n = 3.

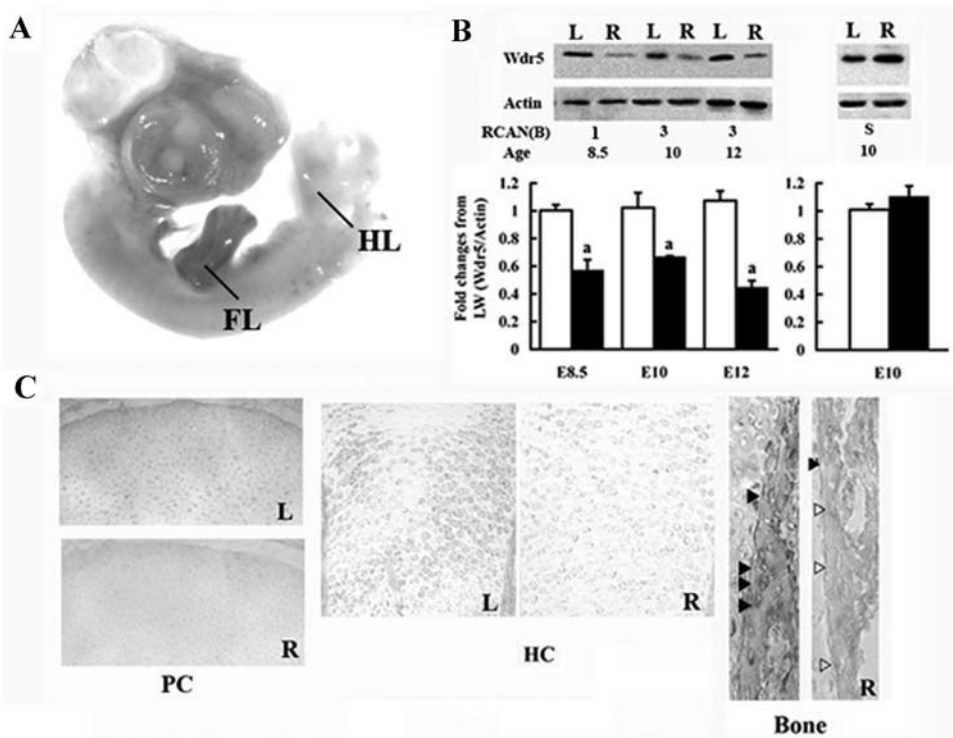

Fig. 2. RCAN-mediated reduction of Wdr5. (*A*) Whole-mount immunohistochemistry analyses demonstrating expression of RCAN protein in the forelimb (FL; in brown). HH stages 18 to 20 (E3) right (R) limb buds were infected with RCAN(B)-3 virus and harvested at HH stage 25 (E5). HL= hindlimbs. (*B*) Western blot analyses and densitometric analyses. Bars represent the ratio of the optical density of Wdr5 normalized to the optical density of actin. Open bars = uninfected left wings; black bars = infected R wings. The results are the mean ± SEM of at least three wings. $^{a}p < .05$ by Student's t test. (*C*) Immunohistochemical analyses demonstrating downregulation of endogenous Wdr5. Embryo limb buds were infected at HH stages 18 to 20 (E3) with RCAN(B)-3 virus and harvested at HH stage 38 (E12) (R). Left wings (L) were used as controls. Representative wings are shown, n = 12. Arrowheads indicate osteoblasts in the bone collar expressing (black) or not expressing (open) Wdr5. PC = proliferating chondrocytes; HC = hypertrophic chondrocytes.

RCAN(B)-S virus. Uninfected left wings served as controls. Embryos then were allowed to develop to HH stages 35 (E8.5), 36 (E10), and 38 (E12). Western blot analyses demonstrate that endogenous Wdr5 levels were significantly reduced by 50% to 60% in the right skeletal elements infected with all RCAN(B)-shWdr5 viruses compared with the uninfected left wings at all time points examined (Fig. 2B). No difference in endogenous Wdr5 protein levels was observed between the infected right wings and uninfected left wings when limb buds were injected with the RCAN(B)-S virus, demonstrating the lack of nonspecific effects of the RCAN(B) virus (Fig. 2B). The efficiency of Wdr5 downregulation in different cell types in the growth plate then was examined by immunohistochemical analyses. Wdr5 levels were markedly decreased in round proliferative chondrocytes and hypertrophic chondrocytes as well in osteoblasts of the right wings infected with all RCAN(B)-shWdr5 viruses compared with the uninfected left wings (Fig. 2C). No difference in endogenous Wdr5 protein levels was observed when limb buds were injected with the RCAN(B)-S virus (data not shown).

Retroviral-mediated expression of shWdr5 impairs endochondral bone development

To explore whether Wdr5 is required for endochondral ossification, HH stage 18 to 20 (E3–3.5) chicken limb buds were injected with high-titer retroviral inoculates. Injections were performed at this time point, prior to chondrogenic condensation of the mesenchymal cells, in order to reduce Wdr5 protein levels in skeletal progenitor cells and to achieve widespread infection of skeletal elements.

Alcian blue and alizarin red staining of whole-mount skeletal preparations of HH stage 35 (E8.5), stage 36 (E10), and stage 38 (E12) embryos shows that infected skeletal elements displayed shorter cartilage elements and decreased mineralization relative to the uninfected left wings (Fig. 3A). This phenotype was observed in 61% of infected wings ($n > 100$). The same phenotype was observed with all viruses used (data not shown). No differences were observed between right wings infected with the RCAN(B)-S virus and uninfected left wings at any time points examined ($n = 20$; Fig. 3A).

Histologic analyses of wings isolated from HH stage 36 (E10) and stage 38 (E12) chick embryos are shown in Fig. 3B. At all time points examined, skeletal elements of infected right wings were shorter than those of the uninfected left wings. Shorter skeletal elements also were observed in HH stage 35 (E8.5) wings (data not shown), suggesting that Wdr5 actions on endochondral bone formation begin at early developmental stages. A delay in vascular invasion (Fig. 3C) and formation of the primary ossification center was observed at HH stage 38 (E12), suggesting delayed endochondral bone formation. Wings infected with the RCAN(B)-S virus displayed a normal phenotype (Fig. 3), confirming that the phenotype observed in infected wings is specific for the RCAN(B)-shWdr5 viruses and is due to reduction of endogenous Wdr5 protein levels. In addition, because the same phenotype was observed when using the three different RCAN(B)-shWdr5 viruses, off-target effects of the shRNAs were excluded. Measurement of the length of the carpometacarpal bones, ulnas, and humeruses confirmed a significant decrease in the overall length of the infected skeletal elements compared with that of uninfected wings (Fig. 3D).

Retroviral-mediated expression of shWdr5 impairs chondrocyte maturation and osteoblast differentiation

Histology of the growth plate of infected wings suggests that a defect in chondrocyte differentiation may account for the overall decrease in the length of the long bones, pointing to an important role of Wdr5 in promoting chondrocyte differentiation. Because the size of the hypertrophic chondrocyte layer is regulated by the rate at which proliferative chondrocytes differentiate, BrdU incorporation analyses were performed. While no difference in the percentage of BrdU-positive nuclei was observed in the BrdU-positive round chondrocytes ($11.4\% \pm 2\%$ SEM in uninfected left wings versus $11.8\% \pm 2.2\%$ SEM in infected right wings, $n = 4$), reduction of Wdr5 led to 42% decrease in the percentage of BrdU-positive cells in the columnar chondrocyte layer of infected wings relative to uninfected left wings 3 hours after BrdU injection ($7.1\% \pm 1.1\%$ SEM in uninfected left wings versus $4.1\% \pm 0.4\%$ SEM in infected right wings; $p < .05$, $n = 4$).

To further characterize this phenotype, the expression of specific chondrocyte and osteoblast genes was assessed by in situ hybridization analyses. At HH stages 36 (E10) and 38 (E12), the distance between the two expression domains of Sox9, which is expressed in proliferating chondrocytes, was smaller, and the expression of ColX, a marker of hypertrophic chondrocytes, was reduced (Fig. 4). Moreover, the distance between the two ColX expression domains was significantly smaller in the infected right wings than in the uninfected left wings, indicating impaired chondrocyte maturation (Fig. 4A). This phenotype was confirmed by a decrease in OP expression, which is expressed in terminally differentiated hypertrophic chondrocytes (Fig. 4A). Decrease in the expression of these chondrocyte specific genes was already observed at HH stage 35 (E8.5; data not shown), prior to bone formation, suggesting that Wdr5 has a direct effect on chondrocyte differentiation. In the infected right wings, the expression of Coll in osteoblasts was decreased compared with the uninfected left wings, indicating that when Wdr5 levels are reduced during limb development, osteoblasts differentiation is impaired as well (Fig. 4A). Confirming the decrease in alizarin red staining, which indicates decreased mineralization (Fig. 3A), the effect of Wdr5 knockdown on osteoblast differentiation also was reflected by a decrease in the mineral deposition, indicated by von Kossa staining, in the bone collar of the infected right wings compared with the uninfected left wings (Fig. 4A). The decrease in the expression of these chondrocyte- and osteoblast-specific genes was quantified by quantitative RT-PCR analyses. In contrast to wings infected with the RCAN(B)-S virus, the expression of these genes was significantly decreased in wings with reduced Wdr5 levels (Fig. 4B).

Retroviral-mediated expression of shWdr5 decreases the expression of Runx2 and misexpression of Runx2 rescues the phenotype induced by Wdr5 shRNA

Wdr5 associates with the β-catenin/Tcf1 response element of the Runx2 promoter and is required for the expression of Runx2 in

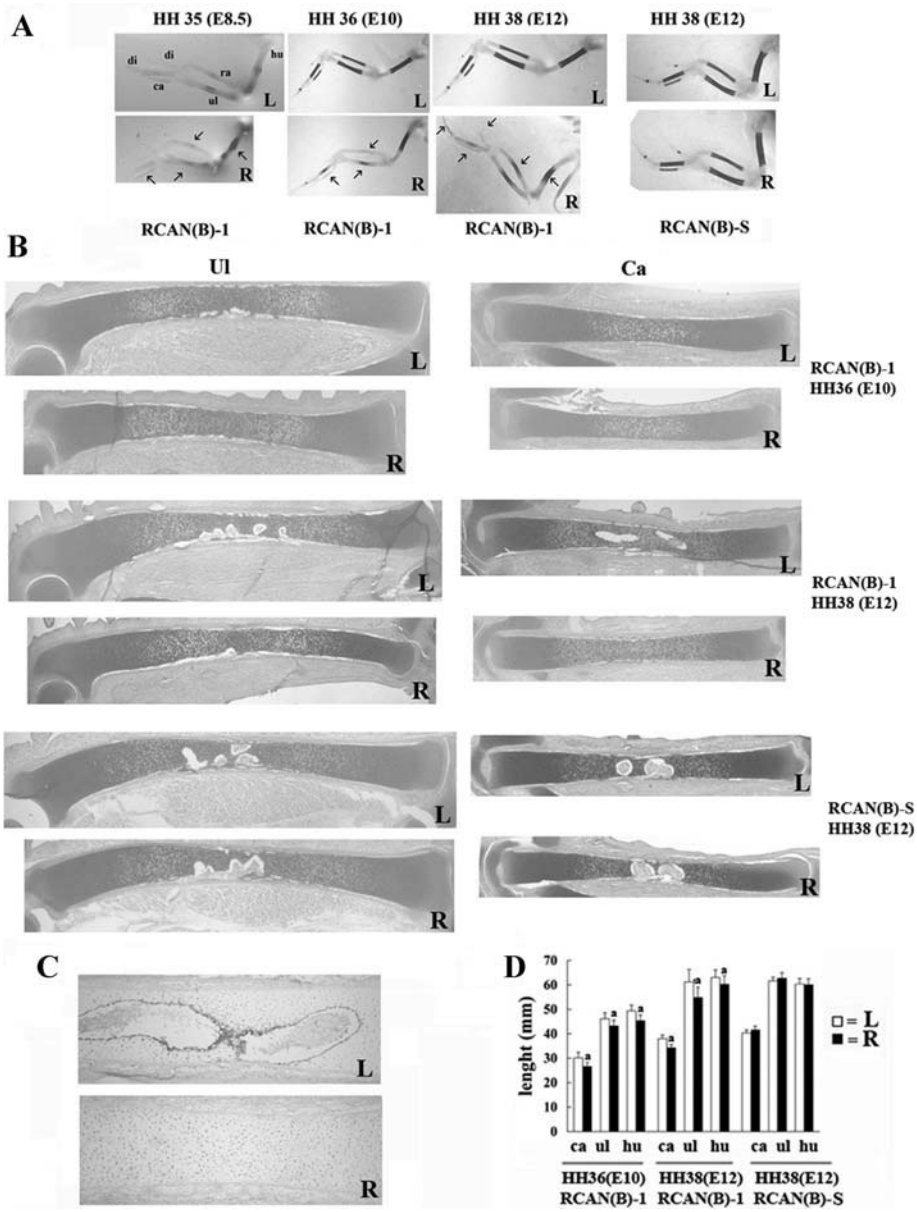

Fig. 3. Reduction of Wdr5 protein impairs endochondral bone development. HH stage 18 to 20 (E3) right limb buds (R) were infected with RCAN(B)-1 or RCAN(B)-S and harvested at stage HH stage 36 (E10) and stage (E12). (*A*) Skeletal preparations stained with alcian blue and alizarin red. Representative wings are shown (n = 16). Arrows indicate the decrease in mineralization. (*B*) Toluidine blue staining (n = 45). Uninfected left wings (L) were used as controls. (*C*) Imunohistochemistry for CD31 showing vascular invasion in the uninfected left HH stage 38 (E12) carpometacarpal bones but not in the infected wings. Representative wings are shown (n = 4). (*D*) Measurement of the length of the carpometacarpal, ulna, and humerus demonstrates a significant reduction in the length of infected bones. Values are expressed as mean ± SEM. [a]$p < .05$ by Student's t test. hu = humerus; ul = ulna; ra = radius; ca = carpometacarpal bones; di = digit.

MC3T3-E1 cells.[36] Thus we asked whether downregulation of Wdr5 in vivo would affect Runx2 expression. When Wdr5 levels are reduced, the expression of Runx2, a critical regulator of chondrocyte hypertrophy and osteoblast differentiation, was decreased significantly in both prehypertrophic chondrocytes and osteoblasts (Fig. 5A).

Because Runx2 is a critical regulator of endochondral bone development, we tested whether impaired Runx2 expression might be responsible for the effects of Wdr5 downregulation on endochondral ossification. To this purpose, we examined whether overexpression of Runx2 could rescue the phenotype observed in the skeletal elements infected with RCAN(B)-shWdr5 viruses. HH stage 18 to 20 (E3–3.5) limb buds were coinfected with an RCAS(A) virus driving the expression of chicken (ch)Runx2, RCAS(A)-chRunx2, in addition to RCAN(B)-1 or with RCAS(A)-GFP plus RCAN(B)-1 (1:1 ratio) and harvested at HH stages 36 (E10) and 38 (E12).

To confirm the efficiency of these coinfection experiments, Runx2 mRNA expression and Wdr5 protein levels were examined first. As shown in Fig. 5C, Runx2 was misexpressed in the growth plate and in the osteoblasts of wings coinfected with RCAS(A)-chRunx2 plus RCAN(B)-1 viruses compared with uninfected wings. In the infected wings, Runx2 also was found expressed in proliferating chondrocytes as well as in adjacent tissues.

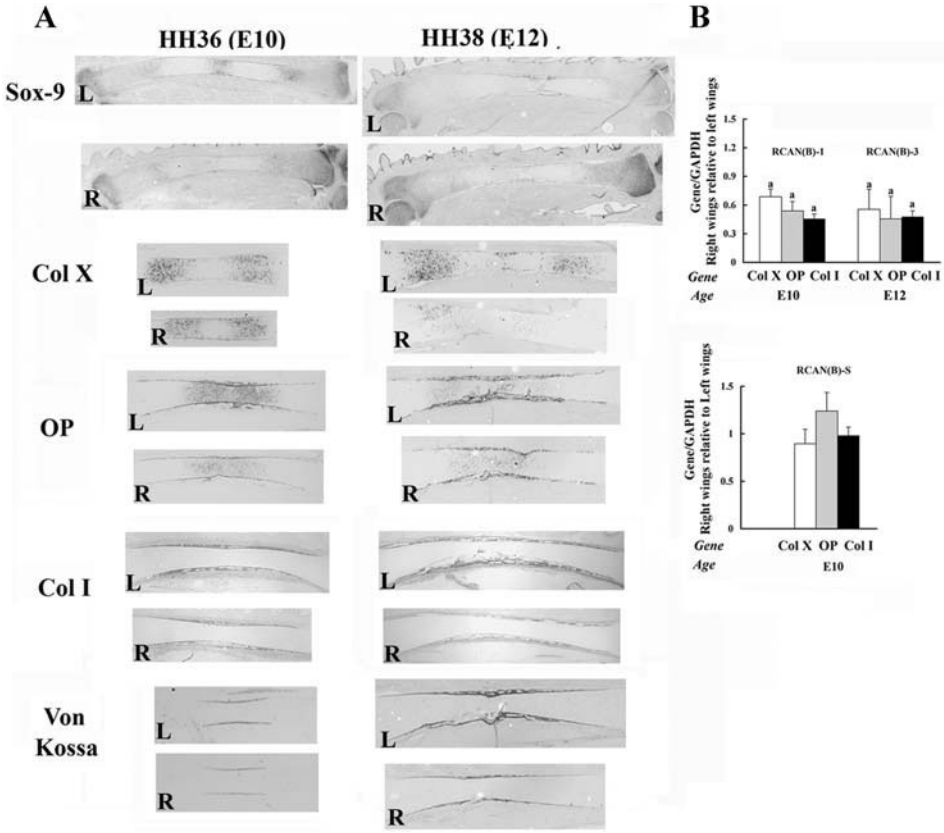

Fig. 4. Reduction of Wdr5 protein impairs chondrocyte and osteoblast differentiation during limb development. HH stage 18 to 20 (E3) right limb buds (R) were infected with RCAN(B)-1 or RCAN(B)-S viruses. (*A*) In situ hybridization analyses and von Kossa staining. Uninfected left wings (L) were used as controls. Representative ulnas are shown, n = 45. (*B*) Quantitative RT-PCR. Expression of all genes was normalized to that of GAPDH in the same sample. Values are expressed as the relative expression of the normalized mRNAs levels of the infected right wings versus that of uninfected left wings. Data are the mean ± SEM of values from three independent experiments. $^{a}p < .05$ by Student's t test.

However, as reported by other investigators,[44] ectopic bone formation was never detected in coinfected wings. Wdr5 protein levels remained significantly downregulated in wings coinfected with RCAS(A)-chRunx2 plus RCAN(B)-1 viruses compared with uninfected left wings (Fig. 5D). This reduction in Wdr5 protein levels was similar to the reduction observed in the RCAN(B)-3-infected wings (Fig. 2C).

Histology of HH stage 36 (E10) and 38 (E12) wings coinfected with RCAS(A)-GFP plus RCAN(B)-1 viruses shows that the infected bones were shorter and displayed delayed chondrocyte maturation and bone formation (Fig. 5E). In contrast, despite Wdr5 downregulation, wings coinfected with RCAS(A)-chRunx2 plus RCAN(B)-1 viruses displayed the same phenotype as the uninfected left wings (0% abnormal wings, n = 24; Fig. 5E). To strengthen these observations, morphometric analyses were performed. As shown in Fig. 5F, retroviral expression of Runx2 rescues the significant decrease in cortical bone seen in wings coinfected with RCAS(A)-GFP plus RCAN(B)-1 viruses.

Confirming the histologic analyses, chondrocyte maturation and thus endochondral ossification were normalized when Runx2 misexpression was accompanied by reduction of Wdr5, as indicated by normal expression pattern of ColX, ColI, and OP (Fig. 5G). Confirming the morphometric analyses, rescue of endochondral bone formation also was evidenced by normal periosteal mineralization in limbs coinfected with RCAS(A)-chRunx2 plus RCAN(B)-1 viruses, as assessed by von Kossa staining (Fig. 5G).

No significant difference in the percentage of BrdU-positive nuclei in the columnar layer of coinfected right wings relative to uninfected left wings (3%, n = 5) was observed, suggesting that the effect of Wdr5 reduction on chondrocyte proliferation was restored.

Discussion

Wdr5 is expressed in proliferating and hypertrophic chondrocytes as well as in the perichondrium and the periosteum of the skeletal elements of chick wings. We have used RCAS vectors driving interfering RNAs successfully to reduce Wdr5 protein levels in these cells. This investigations point to a critical role for Wdr5 in the development of endochondral bones.

RCAS-mediated overexpression of genes in chicken embryos has been used widely to establish many fundamental mechanisms regulating skeletal development.[16–19,45–48] However, in contrast to other animal models, where loss-of-function studies have complemented gain-of-function studies, in the avian model, loss-of-function techniques largely have not been employed.[46–48] Our investigations showing a significant

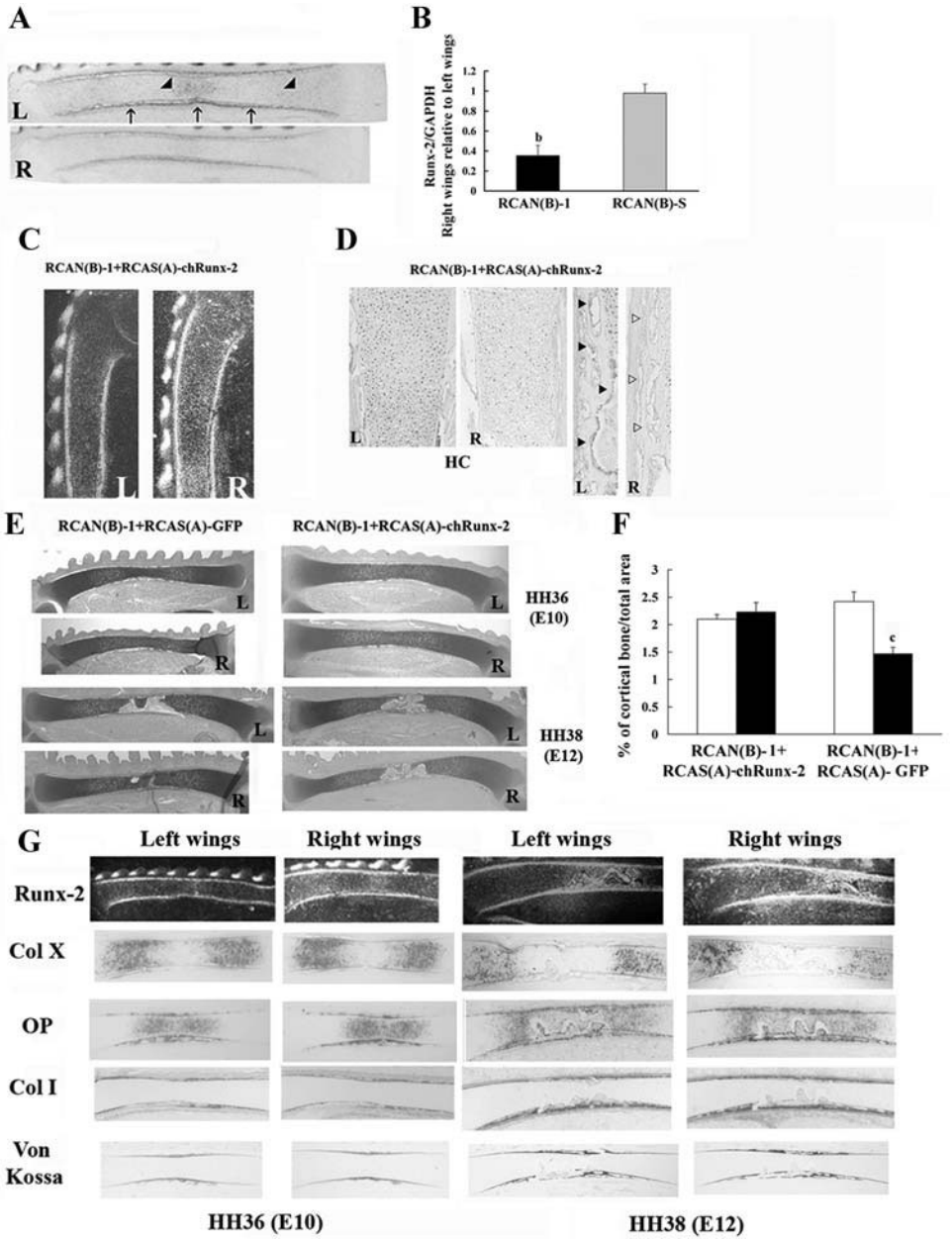

Fig. 5. Runx2 misexpression rescues the endochondral bones phenotype seen when Wdr5 is reduced. HH stage 18 to 20 (E3) right limb buds (R) were infected with RCAN(B)-1 and RCAN(B)-S. Uninfected left wings (L) were used as controls. Embryos were harvested at HH stage 36 (E10). (*A*) In situ hybridization analyses. Representative ulnas are shown, n = 15. Arrow indicates Runx2 expression in the bone collar, and arrowheads indicate Runx2 expression in prehypertrophic and hypertrophic chondrocytes. (*B*) Quantitative RT-PCR. Expression of Runx2 was normalized to that of GAPDH in the same sample. Values are expressed as the relative expression of the normalized mRNA levels of the infected right wings versus that of uninfected left wings. Data are the mean ± SEM of values from three independent experiments. $^{b}p < .001$ by Student's t test. (*C–G*) HH stage 18 to 20 (E3) right limb buds (R) were infected with RCAN(B)-1 plus RCAS(A)-chRunx2 or RCAN(B)-1 plus RCAS(A)-GFP. Embryos were harvested at HH stages 36 (E10) and 38 (E12), and sections of the uninfected left (L) and infected right (R) wings were analyzed by in situ hybridization with a Runx2 probe (*C*), by immunohistochemistry for Wdr5 levels (*D*), and by toludine blue staining for histologic analyses (*E*). HC = hypertrophic chondrocytes. Representative wings are shown, n = 24. (*F*) Quantification of cortical bone. Data are expressed as percentage of cortical bone over total area of the ulna. Data are the mean ± SEM of values from seven RCAN(B)-1 plus RCAS(A)-chRunx2–coinfected wings and from 4 RCAN(B)-1 plus RCAS(A)-GFP–coinfected wings. $^{c}p < .005$ by Student's t test. Open bars = left uninfected ulnas; black bars = right infected ulnae (*G*). In situ hybridization analyses with the indicated probes and von Kossa staining. Representative wings are shown, n = 24.

reduction of Wdr5 protein levels in chondrocytes and osteoblasts of infected wings demonstrate the efficiency of the RCAS system in delivering shRNA to reduce the expression of genes and the feasibility of using this strategy to assess gene function during skeletal development.

Our studies demonstrate that during limb development, Wdr5 is expressed in proliferating and hypertrophic chondrocytes and plays a critical role in regulating chondrocyte maturation. While stable expression of Wdr5 in chondrogenic cells accelerates the program of chondrocyte differentiation in vitro,[33] and

overexpression of Wdr5 in the periosteum leads to accelerated chondrocyte differentiation,[35] whether Wdr5 has in vivo autocrine effects on chondrocytes and whether it is required for chondrocyte differentiation during skeletal development have not been addressed previously. Here we report that when Wdr5 protein levels are reduced by 50% to 60% during development of the skeletal elements of the limbs, Sox9-expressing chondrocytes are formed, but a delay in the progression to prehypertrophic and hypertrophic chondrocytes is observed. Therefore, it is plausible to speculate that while Wdr5 is not essential for the differentiation of skeletal progenitors to proliferative chondrocytes, it is required for the differentiation of proliferating chondrocytes into terminally differentiated chondrocytes.

Mice lacking Runx2 have no osteoblasts and exhibit abnormalities in chondrocyte maturation characterized by decreased chondrocyte hypertrophy and lack of mineralization.[49–53] Overexpression of Runx2 in chondrocytes rescues the chondrocyte phenotype of Runx2 null mice.[54,55] Wdr5 knockdown significantly decreases Runx2 expression in prehypertrophic and hypertrophic chondrocytes, and misexpression of Runx2 reverses the chondrocyte phenotype seen in wings infected with RCAN(B)-shWdr5 viruses. Therefore, it is possible that Wdr5 expressed in proliferating chondrocytes regulates the expression of Runx2 in prehypertrophic cells and, in turn, leads to their differentiation into hypertrophic chondrocytes. However, our studies do not exclude the idea that Runx2 overexpression also may act independently of Wdr5 in rescuing the phenotype caused by Wdr5 knockdown. In addition, the findings that fewer proliferative columnar chondrocytes were observed with Wdr5 downregulation support the hypothesis that round chondrocytes differentiate into columnar chondrocytes and leave the round proliferative layer at a slower rate when Wdr5 levels are reduced and suggest that Wdr5 may be required for the transition of BrdU-positive round chondrocytes to BrdU-positive columnar chondrocytes.

Because several signaling systems and transcription factors interact to coordinate development of endochondral bones, our studies do not exclude the possibility that other signaling molecules involved in chondrocyte maturation may depend on the effects of Wdr5 on this process. Interestingly, the expression of Ihh, a major regulator of chondrocyte maturation known to be regulated by Runx2,[5,56] was not significantly altered in infected wings at HH stage 36 (E10; data not shown). Because the delay in chondrocyte maturation depends on the dosages of Runx2,[56] it is possible that although Wdr5 downregulation decreases Runx2 below levels that are required for chondrocyte hypertrophy to occur, the 60% reduction in the expression of this transcription factor is not sufficient to affect Ihh expression. This hypothesis suggests that either Wdr5 may affect chondrocyte maturation independent of Ihh signaling or that other factors involved in chondrocyte maturation depend on Wdr5 expression. Further studies will be required to confirm this hypothesis.

We have shown recently that overexpression of Wdr5 in osteoblasts regulates chondrocyte differentiation by modulating the expression of Twist-1 in osteoblasts, which, in turn, regulates the expression of FGF18.[35] Therefore, Wdr5 knockdown in osteoblasts also may contribute to the impairment in chondrocyte maturation. However, the findings that stable expression of Wdr5 in ATDC5 cells leads to accelerated hypertrophic differentiation[33] and that impaired chondrocyte differentiation is observed early during skeletal development, prior to the formation of bone collar, suggest direct actions of Wdr5 on chondrocyte maturation. Because a caveat of the RCAS system is that this approach cannot separate direct from indirect actions, mouse genetic studies are needed to address whether Wdr5 directly and/or indirectly affects chondrocyte maturation in vivo. Nonetheless, these studies demonstrate for the first time that in vivo reduction of Wdr5 during skeletal development leads to impaired chondrocyte maturation and that it does so by regulating, at least in part, the expression of Runx2.

Our studies indicate that when Wdr5 levels are reduced, osteoblast differentiation is affected as well. Given the crosstalk between chondrocytes and osteoblasts and the limitations of the RCAS approach in discriminating between Wdr5 requirements for chondrocytes and osteoblasts, these studies do not exclude the possibility that the impairment observed in osteoblast differentiation may be a consequence of impaired hypertrophic differentiation. However, previous studies are also consistent with the hypothesis that Wdr5 has an independent effect on osteoblast differentiation. Stable expression of Wdr5 in MC3T3-E1 cells, which are derived from murine calvarial bones, and in type I collagen–expressing osteoblasts accelerates osteoblast differentiation,[32,34] and silencing of Wdr5 in MC3T3-E1 cells arrests osteoblast differentiation, an effect that mirrors that seen in infected wings.[36] In addition, Wdr5 also associates with the Runx2 promoter in the context of intact chromatin in these cells, and its recruitment to the Runx2 promoter is significantly decreased in MC3T3-E1 cells with Wdr5 knockdown, which also have decreased Runx2 mRNA.[36,57]

Hence, although we do not rule out indirect actions of Wdr5, our data do not exclude the hypothesis that Wdr5 might directly affect both chondrocyte and osteoblast differentiation. In summary, these studies indicate that in vivo Wdr5 is required for endochondral bone formation and provide evidence that Wdr5 exerts these effects at least in part by regulating the expression of Runx2. Most significantly, the findings that impaired endochondral bone formation is observed with a 50% to 60% decrease in endogenous Wdr5 levels strongly suggest that Wdr5 plays a critical role in skeletal biology.

Disclosures

All the authors state that they have no conflicts of interest.

Acknowledgments

We thank Dr Marie Demay for helpful discussion. This work was supported by Grant DK 076093 to FG from the National Institutes of Health.

References

1. Olsen BR, Reginato AM, Wang W. Bone development. Annu Rev Cell Dev Biol. 2000;16:191–220.

2. Karsenty G. The genetic transformation of bone biology. Genes Dev. 1999;13:3037–3051.
3. Wagner EF, Karsenty G. Genetic control of skeletal development. Curr Opin Genet Dev. 2001;11:527–532.
4. Karsenty G, Wagner EF. Reaching a genetic and molecular understanding of skeletal development. Dev Cell. 2002;2:389–406.
5. Kronenberg HM. Developmental regulation of the growth plate. Nature. 2003;423:332–336.
6. Provot S, Schipani E. Molecular mechanisms of endochondral bone development. Biochem Biophys Res Commun. 2005;328:658–665.
7. Canalis E, Economides AN, Gazzerro E. Bone morphogenetic proteins, their antagonists, and the skeleton. Endocr Rev. 2003;24:218–235.
8. Ornitz DM. FGF signaling in the developing endochondral skeleton. Cytokine Growth Factor Rev. 2005;16:205–213.
9. Hartmann C. A Wnt canon orchestrating osteoblastogenesis. Trends Cell Biol. 2006;16:151–158.
10. Schipani E, Provot S. PTHrP, PTH, and the PTH/PTHrP receptor in endochondral bone development. Birth Defects Res C Embryo Today. 2003;69:352–362.
11. Mariani FV, Martin GR. Deciphering skeletal patterning: clues from the limb. Nature. 2003;423:319–325.
12. Stern CD. The chick; a great model system becomes even greater. Dev Cell. 2005;8:9–17.
13. Stern CD. The chick embryo–past, present and future as a model system in developmental biology. Mech Dev. 2004;121:1011–1013.
14. Tickle C. The contribution of chicken embryology to the understanding of vertebrate limb development. Mech Dev. 2004;121: 1019–1029.
15. Hughes SH. The RCAS vector system. Folia Biol (Praha). 2004;50:107–119.
16. Hartmann C, Tabin CJ. Dual roles of Wnt signaling during chondrogenesis in the chicken limb. Development. 2000;127:3141–3159.
17. Duprez D, Bell EJ, Richardson MK, et al. Overexpression of BMP-2 and BMP-4 alters the size and shape of developing skeletal elements in the chick limb. Mech Dev. 1996;57:145–157.
18. Pizette S, Niswander L. BMPs are required at two steps of limb chondrogenesis: formation of prechondrogenic condensations and their differentiation into chondrocytes. Dev Biol. 2000;219:237–249.
19. Eames BF, Sharpe PT, Helms JA. Hierarchy revealed in the specification of three skeletal fates by Sox9 and Runx2. Dev Biol. 2004;274: 188–200.
20. Tavares AT, Izpisuja-Belmonte JC, Rodriguez-Leon J. Developmental expression of chick twist and its regulation during limb patterning. Int J Dev Biol. 2001;45:707–713.
21. Kawakami Y, Capdevila J, Buscher D, Itoh T, Rodriguez Esteban C, Izpisua Belmonte JC. WNT signals control FGF-dependent limb initiation and AER induction in the chick embryo. Cell. 2001;104: 891–900.
22. Kawakami Y, Esteban CR, Matsui T, Rodriguez-Leon J, Kato S, Belmonte JC. Sp8 and Sp9, two closely related buttonhead-like transcription factors, regulate Fgf8 expression and limb outgrowth in vertebrate embryos. Development. 2004;131:4763–4774.
23. Abzhanov A, Cordero DR, Sen J, Tabin CJ, Helms JA. Cross-regulatory interactions between Fgf8 and Shh in the avian frontonasal prominence. Congenit Anom (Kyoto). 2007;47:136–148.
24. Tickle C. Limb development: an international model for vertebrate pattern formation. Int J Dev Biol. 2000;44:101–108.
25. Tickle C, Munsterberg A. Vertebrate limb development–the early stages in chick and mouse. Curr Opin Genet Dev. 2001;11:476–481.
26. Provot S, Kempf H, Murtaugh LC, et al. Nkx3.2/Bapx1 acts as a negative regulator of chondrocyte maturation. Development. 2006;133:651–662.
27. Gordon CT, Rodda FA, Farlie PG. The RCAS retroviral expression system in the study of skeletal development. Dev Dyn. 2009.
28. Neer EJ, Smith TF. G protein heterodimers: new structures propel new questions. Cell. 1996;84:175–178.
29. Smith TF, Gaitatzes C, Saxena K, Neer EJ. The WD repeat: a common architecture for diverse functions. Trends Biochem Sci. 1999;24:181–185.
30. Neer EJ, Smith TF. A groovy new structure. Proc Natl Acad Sci U S A. 2000;97:960–962.
31. Neer EJ, Schmidt CJ, Nambudripad R, Smith TF. The ancient regulatory-protein family of WD-repeat proteins. Nature. 1994;371:297–300.
32. Gori F, Divieti P, Demay MB. Cloning and characterization of a novel WD-40 repeat protein that dramatically accelerates osteoblastic differentiation. J Biol Chem. 2001;276:46515–46522.
33. Gori F, Demay MB. BIG-3, a novel WD-40 repeat protein, is expressed in the developing growth plate and accelerates chondrocyte differentiation in vitro. Endocrinology. 2004;145:1050–1054.
34. Gori F, Friedman LG, Demay MB. Wdr5, a WD-40 protein, regulates osteoblast differentiation during embryonic bone development. Dev Biol. 2006;295:498–506.
35. Gori F, Zhu ED, Demay MB. Perichondrial expression of Wdr5 regulates chondrocyte proliferation and differentiation. Dev Biol. 2009.
36. Zhu ED, Demay MB, Gori F. Wdr5 is essential for osteoblast differentiation. J Biol Chem. 2008;283:7361–7367.
37. Nelson CE, Morgan BA, Burke AC, et al. Tabin C. Analysis of Hox gene expression in the chick limb bud. Development. 1996;122:1449–1466.
38. Church VL, Francis-West P. Wnt signalling during limb development. Int J Dev Biol. 2002;46:927–936.
39. Boulet AM, Moon AM, Arenkiel BR, Capecchi MR. The roles of Fgf4 and Fgf8 in limb bud initiation and outgrowth. Dev Biol. 2004;273:361–372.
40. Crossley PH, Minowada G, MacArthur CA, Martin GR. Roles for FGF8 in the induction, initiation, and maintenance of chick limb development. Cell. 1996;84:127–136.
41. Morgan BA, Fekete DM. Manipulating gene expression with replication-competent retroviruses. Methods Cell Biol. 1996;51:185–218.
42. Logan M, Tabin C. Targeted gene misexpression in chick limb buds using avian replication-competent retroviruses. Methods. 1998;14: 407–420.
43. Livak KJ, Schmittgen TD. Analysis of relative gene expression data using real-time quantitative PCR and the 2(-Delta Delta C(T)) Method. Methods. 2001;25:402–408.
44. Stricker S, Fundele R, Vortkamp A, Mundlos S. Role of Runx genes in chondrocyte differentiation. Dev Biol. 2002;245:95–108.
45. Buxton P, Edwards C, Archer CW, Francis-West P. Growth/differentiation factor-5 (GDF-5) and skeletal development. J Bone Joint Surg Am. 2001;83-A (Suppl 1Pt 1): S23–30.
46. Harpavat S, Cepko CL. RCAS-RNAi: a loss-of-function method for the developing chick retina. BMC Dev Biol. 2006;6:2.
47. Bron R, Eickholt BJ, Vermeren M, Fragale N, Cohen J. Functional knockdown of neuropilin-1 in the developing chick nervous system by siRNA hairpins phenocopies genetic ablation in the mouse. Dev Dyn. 2004;230:299–308.
48. Hashimoto T, Zhang XM, Chen BY, Yang XJ. VEGF activates divergent intracellular signaling components to regulate retinal progenitor cell proliferation and neuronal differentiation. Development. 2006;133: 2201–2210.
49. Otto F, Thornell AP, Crompton T, et al. Owen MJ. Cbfa1, a candidate gene for cleidocranial dysplasia syndrome, is essential for osteoblast differentiation and bone development. Cell. 1997;89:765–771.

50. Komori T. Requisite roles of Runx2 and Cbfb in skeletal development. J Bone Miner Metab. 2003;21:193–197.

51. Komori T. Regulation of osteoblast differentiation by transcription factors. J Cell Biochem. 2006;99:1233–1239.

52. Komori T, Yagi H, Nomura S, et al. Targeted disruption of Cbfa1 results in a complete lack of bone formation owing to maturational arrest of osteoblasts. Cell. 1997;89:755–764.

53. Ducy P, Zhang R, Geoffroy V, Ridall AL, Karsenty G. Osf2/Cbfa1: a transcriptional activator of osteoblast differentiation. Cell. 1997;89: 747–754.

54. Takeda S, Bonnamy JP, Owen MJ, Ducy P, Karsenty G. Continuous expression of Cbfa1 in nonhypertrophic chondrocytes uncovers its ability to induce hypertrophic chondrocyte differentiation and partially rescues Cbfa1-deficient mice. Genes Dev. 2001;15:467–481.

55. Ueta C, Iwamoto M, Kanatani N, et al. Skeletal malformations caused by overexpression of Cbfa1 or its dominant negative form in chondrocytes. J Cell Biol. 2001;153:87–100.

56. Yoshida CA, Yamamoto H, Fujita T, et al. Runx2 and Runx3 are essential for chondrocyte maturation, and Runx2 regulates limb growth through induction of Indian hedgehog. Genes Dev. 2004; 18:952–963.

57. Gori FDMB. Wdr5 is required for chromatin modifications at the Runx-2 promoter. J Bone Miner Res. 2008;23:S383.